

# Extending RAIM with a Gaussian Mixture of Opportunistic Information

Wenjie Liu and Panos Papadimitratos

*Networked Systems Security Group, KTH Royal Institute of Technology, Sweden*

## BIOGRAPHY

**Wenjie Liu** received the B.Eng. degree from the University of Electronic Science and Technology of China, Chengdu, China, in 2019, and the M.Phil. degree from The Chinese University of Hong Kong, Shenzhen, in 2021. He is currently pursuing the Ph.D. degree with the School of Electrical Engineering and Computer Science, KTH Royal Institute of Technology. He was a Visiting Student/an Exchange Student at Peking University and the Harbin Institute of Technology and interned at the Intel Asia-Pacific Research and Development Center. His research interests mainly include security and privacy.

**Panos Papadimitratos** is a professor with the School of Electrical Engineering and Computer Science (EECS) at KTH Royal Institute of Technology, Stockholm, Sweden, where he leads the Networked Systems Security (NSS) group. He earned his Ph.D. degree from Cornell University, Ithaca, New York, in 2005. His research agenda includes a gamut of security and privacy problems, with an emphasis on wireless networks. He is an IEEE Fellow, an ACM Distinguished Member, and a Fellow of the Young Academy of Europe.

## ABSTRACT

Global navigation satellite systems (GNSSs) are indispensable for various applications, but they are vulnerable to spoofing attacks. The original receiver autonomous integrity monitoring (RAIM) was not designed for securing GNSS. In this context, RAIM was extended with wireless signals, termed signal of opportunitys (SOPs), or onboard sensors, typically assumed benign. However, attackers might also manipulate wireless networks, raising the need for a solution that considers untrustworthy SOPs. To address this, we extend RAIM by incorporating all *opportunistic information*, i.e., measurements from terrestrial infrastructures and onboard sensors, culminating in one function for robust GNSS spoofing detection. The objective is to assess the likelihood of GNSS spoofing by analyzing locations derived from extended RAIM solutions, which include location solutions from GNSS pseudorange subsets and wireless signal subsets of untrusted networks. Our method comprises two pivotal components: subset generation and location fusion. Subsets of ranging information are created and processed through positioning algorithms, producing temporary locations. Onboard sensors provide speed, acceleration, and attitude data, aiding in location filtering based on motion constraints. The filtered locations, modeled with uncertainty, are fused into a composite likelihood function normalized for GNSS spoofing detection. Theoretical assessments of GNSS-only and multi-infrastructure scenarios under uncoordinated and coordinated attacks are conducted. The detection of these attacks is feasible when the number of benign subsets exceeds a specific threshold. A real-world dataset from the Kista Science City area is used for experimental validation. Comparative analysis against baseline methods shows a significant improvement in detection accuracy achieved by our Gaussian Mixture RAIM approach. Moreover, we discuss leveraging RAIM results for plausible location recovery. The theoretical analysis and experimental validation underscore the efficacy of our spoofing detection approach.

## I. INTRODUCTION

Authentication mechanisms (GMV, 2023b, 2023a) improve the security of next-generation global navigation satellite system (GNSS), making it more challenging for attackers to manipulate the location and time of victims (Goodin, 2022; Werner, 2022; Spanghero & Papadimitratos, 2023). However, it is crucial to recognize that authentication has limitations against sophisticated spoofing techniques, such as relay and replay attacks occurring at both signal and message levels. They can not only record signals at one location and replay them at another location later, but also make the forged signal appear to arrive earlier than the actual signal (e.g., distance-decreasing attacks) (Zhang & Papadimitratos, 2019a; Lenhart, Spanghero, & Papadimitratos, 2022; Zhang, Larsson, & Papadimitratos, 2022). Then, attackers control one or more satellites of their choice and gradually induce location deviation on the victim receiver (Shen, Won, Chen, & Chen, 2020; Gao & Li, 2022). In essence, the focus should shift towards mitigating evolving threats, including slow-varying relay and replay attacks and potential exploits at the physical layer of wireless signals (Wesson, Rothlisberger, & Humphreys, 2012; Zhang, Tuhin, & Papadimitratos, 2015; Anderson et al., 2017; S. Liu et al., 2021) and overall weed out signals manipulated by the adversary.

Receiver autonomous integrity monitoring (RAIM) (Brown, 1992) is originally an approach to assess the integrity of GNSS signals, but it is also commonly used to detect and possibly exclude one or more satellite signals that are faulty or possibly spoofed (Zhang et al., 2015; Zhang & Papadimitratos, 2021). RAIM compares observed pseudoranges with expected values, and based on redundant satellite combinations, it generates the corresponding GNSS-computed locations. It relies solely on the

GNSS infrastructure, offering the advantage of independence from other infrastructures, especially when leveraging multiple constellations (Zhang & Papadimitratos, 2021). However, its inherent limitation becomes apparent when facing strong adversary attacks, targeting a significant subset of satellite signals: RAIM (Brown, 1992) needs a minimum of 5 available (unaffected by the attack) satellites to detect a single fault or at least 6 satellites to isolate it.

On the other hand, GNSS receivers are commonly integrated into mobile computing platforms equipped with diverse network interfaces and onboard sensors (Shen et al., 2020; Kassas, Khalife, Abdallah, & Lee, 2022; Olinger, Sciancalepore, Ibrahim, & Di Pietro, 2022). These platforms not only receive signals from satellites but also capture signal of opportunitys (SOPs) from cellular network base stations (BSs), wireless access points (APs), and other terrestrial networking infrastructures. By leveraging redundant sensor information and SOPs, i.e., *opportunistic information*, it is possible to extend RAIM mechanisms (Khanafseh et al., 2014; Maaref & Kassas, 2021). RAIM with inertial sensor coupling (Khanafseh et al., 2014) introduced a test statistic utilizing a weighted norm of a residual vector, representing the difference between actual global positioning system (GPS) measurements and predictions, with a threshold determining the hypothesis test. SOP-based RAIM (Maaref & Kassas, 2021) utilizes cellular networks as sources of SOPs and an inertial measurement unit (IMU), offering a relatively accurate backup location when GNSS signals are unreliable.

The aforementioned methods (including our previous work (W. Liu & Papadimitratos, 2023)) assume that SOPs are benign. Onboard sensors can be trusted as long as the GNSS receiver-bearing platform is not hacked, and it is reasonable to assume in certain settings that SOPs are not adversarial. However, the challenge arises when parts of the terrestrial infrastructures are not benign or their signaling/messaging is under attack. For example, attackers can break the authentication protocols of wireless networks, such as WPA2 (Vanhoef & Piessens, 2017), replay signals, or deploy rogue 4G/5G/Wi-Fi stations (Shaik, Borgaonkar, Park, & Seifert, 2018; Saedi et al., 2020; Yan et al., 2022). To the best of our knowledge, the detection of GNSS attacks using untrusted *opportunistic information* remains unsolved. Therefore, our work extends RAIM by integrating all *opportunistic information*, including terrestrial wireless signals and onboard sensors, while considering the possibility of untrustworthy wireless signals.

In this paper, we propose and investigate an extended RAIM-based GNSS spoofing detection algorithm that combines signals from GNSS satellites, available terrestrial networks (e.g., Wi-Fi and cellular), and onboard inertial sensors. The key idea is to consider different combinations of GNSS pseudoranges and ranging information extracted from untrusted network infrastructures and derive multiple location solutions with uncertainty in a RAIM manner. These solutions are then aggregated into a Gaussian mixture function to evaluate the correctness of the GNSS location. It is important to note that apart from spoofing the GNSS location, we assume the attacker has rogue Wi-Fi and cellular stations, or replays legitimate terrestrial wireless network traffic.

Our scheme consists of two key components: subset generation for temporary position computations and location fusion for spoofing detection. The first component of our scheme collects ranging information in real-time from multiple infrastructures including GNSS satellites and terrestrial infrastructures. For individual infrastructures, subsets are generated as combinations of ranging information, with a subset size from the minimal measurements required by the positioning algorithm to the maximum. Then, a positioning algorithm (multilateration, nonlinear least squares, etc.) computes temporary locations for each subset and infrastructure individually. The second component uses onboard sensors to collect speed, acceleration, and attitude data, which is used to assist in filtering the temporary locations obtained from the first component. The filtering process smoothens the locations according to motion constraints, and the uncertainty of the filtered locations is modeled as variance based on the dilution of precision or the residuals between the historical temporary locations and filtered locations. The filtered locations are then fused with uncertainty, and the composite likelihood function is normalized to obtain the ultimate likelihood function used for GNSS spoofing detection.

Within our experiments and analysis, we initially conduct a theoretical assessment of GNSS-only and multi-infrastructure scenarios under two types of attacks: uncoordinated attacks and coordinated attacks. Coordinated attacks involve the coordinated manipulation of multiple pseudoranges and other ranging information for a specifically designed spoofing path, presenting a higher level of complexity, and uncoordinated attacks otherwise. Our analysis reveals that the proposed RAIM extension generates a significantly larger set of subsets for cross-validating locations, effectively countering attacks; thus raising the bar for the attacker needing to intrude or attack different (all) types of terrestrial infrastructures and GNSS. We evaluate our method using a real-world dataset, collected at the Kista Science City, encompassing ground truth location traces, pseudoranges, acceleration, attitude, cellular names, Wi-Fi names, and received signal strength indicator (RSSI) measurements. Through comparative analysis with state-of-the-art baseline methods, we find improved detection accuracy achieved by our method.

In conclusion, the novelty is to handle untrusted *opportunistic information* and propose a Gaussian mixture RAIM for detecting GNSS spoofing attacks. We discuss how to use the results from RAIM towards recovering a plausible position, in Sec. V. Additionally, we provide a theoretical analysis of the detection in Sec. V-D and demonstrate the performance of our spoofing detection approach in Sec. VI.

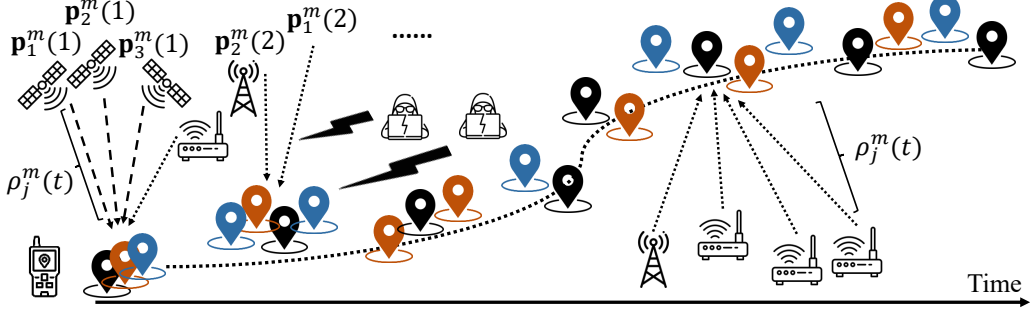


Fig. 1: System and adversary model illustration.

## II. RELATED WORK

### A. GNSS Spoofing vs Meaconing

GNSS spoofing generates false but correctly formatted GNSS signals (Humphreys et al., 2008; Sathaye, Strohmeier, Lenders, & Ranganathan, 2022). It is difficult to detect as it can usually cause subtle discrepancies in timing, strength, and direction which most modern receivers can not distinguish. Despite the implementation of GNSS authentication measures (GMV, 2023b, 2023a) for countering spoofing, attackers employ replaying techniques to mimic genuine GNSS signals (Maier, Frankl, Blum, Eissfeller, & Pany, 2018; Lenhart et al., 2022), or distance-decreasing attack (Zhang & Papadimitratos, 2019a; Zhang et al., 2022) to alter signals to create the illusion of an earlier arrival compared to their actual arrival. Shen et al. (2020); Gao and Li (2022) focus on a slowly varying algorithm to evade tightly-coupled GNSS/IMU systems, while Gao and Li (2023) explores two time-based gradual spoofing algorithms designed for GNSS clock in the navigation message. Moreover, a significant concern lies in the adaptability of attackers utilizing versatile software-defined radios (SDRs). SDRs not only enable GNSS spoofing, but also pose a threat to other SOP navigation, including Wi-Fi and cellular networks (Shi, Davaslioglu, & Sagduyu, 2020). This multidimensional threat underscores the need for comprehensive countermeasures.

### B. RAIM Protecting GNSS

RAIM traditionally relies on redundant information and consistency checks among pseudoranges or position solutions obtained from subsets of visible satellites. One significant approach employs statistical hypothesis testing techniques, where residual errors from the positioning least-squares method are scrutinized to identify faulty measurements, and then testing is applied to assess the reliability of these measurements (Joerger, Chan, & Pervan, 2014). Clustering RAIM, as proposed in Zhang et al. (2015), integrates RAIM with a clustering algorithm to achieve a binary classification of location solutions from various pseudorange subsets. Their follow-up work (Zhang & Papadimitratos, 2019b) digs into multi-constellation situations and (Zhang & Papadimitratos, 2021) proposes a faster fault exclusion algorithm considering performance trade-off. Extended Kalman filter (EKF)-combined RAIM in Khanafseh et al. (2014); Roysdon and Farrell (2017) detects and eliminates outliers in GPS and inertial sensors navigation systems using a sliding window filter. To extend RAIM with more constellations, advanced RAIM (Blanch et al., 2015) is proposed to use GPS, Galileo, and others for fault exclusion. Recently, SOP techniques have also been explored. The work (Maaref & Kassas, 2021) focuses on RAIM using cellular signals and proposes a EKF-based navigation framework that incorporates the vehicle's kinematics model, clock errors, and cellular pseudorange measurements. None of these methods account for RAIM using untrusted opportunistic information.

## III. SYSTEM MODEL AND ADVERSARY

### A. System Model

We examine a mobile GNSS platform depicted in Fig. 1, which can be a device such as a smartphone, car, or drone. The platform is equipped with modules that provide opportunistic information, including wireless signals from network interfaces, such as Wi-Fi and cellular networks, and motion measurements from onboard sensors, such as IMUs and wheel speed sensors. However, in some cases, GNSS satellites and network data may be unavailable, under attack, or have an unacceptable latency, leading to the provision of incorrect ranging information (e.g., pseudoranges and RSSI). On the other hand, the IMU provides three-axis acceleration measurements at a high frequency, and wheel speed sensors or pedometers provide speed measurements in certain situations, such as in vehicles or smartphones.

It is worth noting that opportunistic information is not specifically designed for localization, and is unintendedly available. In benign environments where the mobile platform is moving and navigating on a path, the estimated GNSS location would be consistent with the opportunistic information. However, when an adversary launches an attack, the GNSS-derived results could deviate from the actual location and be inconsistent with opportunistic information.

$\mathbf{p}_c(t) \in \mathbb{R}^3$  denotes the receiver actual location at time  $t$ , to be determined through positioning. GNSS and network interfaces, namely Wi-Fi and cellular, can provide ranging information from either GNSS or terrestrial networks (pseudoranges or SOPs):  $\rho_j^m(t), j = 1, 2, \dots, J_m, m = 1, 2, \dots, M$  is ranging information at time  $t$ , where  $J_m$  is the total number of *anchors* from the  $m$ th infrastructure (i.e., GNSS satellites/BSs/APs) providing ranging information and  $M$  is the total number of infrastructures;  $t = 1, 2, \dots, N$  and  $N$  is the last time index. Correspondingly,  $\mathbf{p}_j^m(t) \in \mathbb{R}^3$  is the location of the anchor for ranging information  $\rho_j^m(t)$ , which is known. Meanwhile, onboard sensors provide motion measurements, i.e., speed  $\mathbf{v}(t)$  and acceleration  $\mathbf{a}(t)$ . They are updated as discrete time series at different frequencies.

### B. Adversary

The adversary in Fig. 1 spoofs GNSS and network signals to force the mobile platform to get incorrect ranging information, in order to manipulate it into estimating an incorrect location. The adversary also possesses knowledge of the victim's actual location with sufficient low observational error. To carry out the attack, the adversary uses SDR devices with state-of-the-art GNSS and network infrastructure spoofing algorithms, to falsify some wireless signals of certain anchors (i.e., GNSS satellites, BSs, and APs) (Shi et al., 2020; Lenhart et al., 2022), causing a designed gradual deviation from the actual location.

**Assumptions.** We assume the attacker is a sophisticated GNSSspoof, rather than an unskillful jammer, with the capability to track satellites and generate multiple adversarial signals. It can also deploy rogue APs or BSs. The terrestrial infrastructures are assumed to implement standardized and regularly updated security mechanisms, including authentication. Consequently, we assume the attacker uses replay/relay-like attacks (Shi et al., 2020). Additionally, we assume that the attacker lacks physical control over the victim, ensuring the security of the procedure for deriving locations from pseudoranges and opportunistic information.

**Attack strategy.** The attacker uses replay/relay-like attacks and rogue APs/BSs for GNSS and network infrastructures and designs a trajectory for the spoofed locations that carefully mimics part of the wireless signals for the mobile platform to cause subtle yet significant deviations. The attacker will control part of the anchors (Ranganathan, Ólafsdóttir, & Capkun, 2016; Gao & Li, 2022) and use various trajectory strategies, such as gradual deviating (Shen et al., 2020) and path drift (Narain, Ranganathan, & Noubir, 2019), to hinder the victim's ability to detect the attack on GNSS signals. These tactics aim to manipulate the mobile platform's position estimation and deceive the victim into believing that they are following the attacker-designed path (as the result of the attack).

## IV. PROBLEM STATEMENT

Our goal is to analyze whether all computed RAIM positions are consistent with each other through using opportunistic information and accordingly make a decision on whether the current GNSS location is the result of a spoofing attack. We care most about safeguarding the GNSS position because it is usually the most accurate location provider. We would like to provide a likelihood estimate of whether the GNSS system is under attack and maximize the accuracy of GNSS spoofing detection. We focus on the design of the extended RAIM.

At a time  $t$ , we use data  $\{\mathbf{p}_j^m(i), \rho_j^m(i), \mathbf{v}(i), \mathbf{a}(i)\}$  for  $j = 1, 2, \dots, J_m, m = 1, 2, \dots, M$  and  $0 < i < t$ , to determine whether the current GNSS position is affected by an attack. We formulate two hypotheses:

- $H_0$ : GNSS is not under attack.
- $H_1$ : GNSS is under attack.

The decision at time  $t$  is denoted as  $\hat{H}(t) \in \{H_0, H_1\}$ . We define true positive for  $t$  as  $\mathbb{I}\{\hat{H}(t) = H_1 | H_1\} = 1$  and false positive as  $\mathbb{I}\{\hat{H}(t) = H_1 | H_0\} = 1$ , where the indicator function  $\mathbb{I}\{A|B\}$  takes value 1 if A holds on condition of B. We denote the total number of positives as  $N_p$ , the number of true positives as  $N_{TP}$ , and the number of false positives as  $N_{FP}$ . Then, the true positive probability for the period  $0 < t \leq N$  is  $P_{TP}(\hat{H}(t)) = P(\hat{H}(t) = H_1 | H_1) = \frac{N_{TP}}{N_p}$  and the Type I error (false positive) probability is  $P_{FP}(\hat{H}(t)) = P(\hat{H}(t) = H_1 | H_0) = \frac{N_{FP}}{N - N_p}$ . The objective is to maximize the true positive probability  $P_{TP}$  of attack detection, given  $P_{FP_{max}}$ :

$$\begin{aligned} \max \quad & P_{TP}(\hat{H}(t)) \\ \text{s.t.} \quad & P_{FP}(\hat{H}(t)) \leq P_{FP_{max}} \end{aligned}.$$

## V. PROPOSED SCHEME

### A. Scheme Outline

We propose a Gaussian mixture RAIM approach for detecting GNSS spoofing by utilizing multiple information sources, such as GNSS pseudoranges, SOPs, speed, acceleration, and attitude. Fig. 2 provides a high-level overview of our GNSS spoofing detection system, which collects input data from GNSS and other opportunistic information sources. Creating subsets of ranging information based on different infrastructures allows us to accommodate variations in the data characteristics of each information source, including considerations of average distance, variance, and accuracy of distance. Utilizing the corresponding positioning algorithm, we compute temporary locations for each subset, which are then “de-noise” using an onboard sensor-assisted filter and modeled with a statistical tool to estimate their uncertainty. By comparing the fused locations with uncertainty to the original GNSS computed location, we can assess the likelihood of GNSS spoofing.

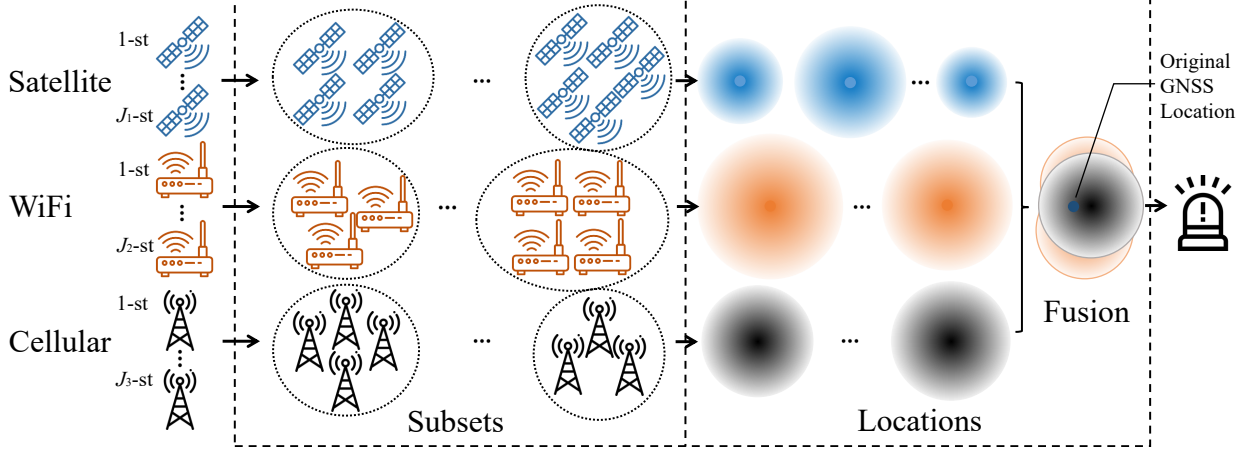


Fig. 2: System overview of Gaussian mixture RAIM.

**Algorithm 1** Extending RAIM with a Gaussian mixture of opportunistic information

---

**Input**  $\{\mathbf{p}_j^m(t), \rho_j^m(t), \mathbf{v}(t), \mathbf{a}(t)\}$  for  $j = 1, 2, \dots, J_m$  and  $m = 1, 2, \dots, M$   
**Parameter**  $\Lambda$   
**Output** *IsAttack*

```

1: for  $t = 1, t++, t \leq N$  do ▷ Time index
2:   for  $l = 1, l++, l \leq L$  do ▷ Loop through all subsets
3:      $\mathbf{p}_l(t) \leftarrow$  Eq. (1), (2), or (3) ▷ Positioning algorithms
4:      $\hat{\mathbf{p}}_l(t) = \mathbf{W}_l \leftarrow$  Eq. (7) ▷ Local polynomial regression
5:      $\sigma_l(t) \leftarrow$  Eq. (9) ▷ Uncertainty modelling
6:      $f_{l,t}(\mathbf{p}) = \frac{1}{\sigma_l(t)\sqrt{2\pi}} \exp\left(-\frac{1}{2} \frac{(\mathbf{p} - \hat{\mathbf{p}}_l(t))^2}{\sigma_l(t)^2}\right)$  ▷ Probability density function
7:   end for
8:    $f_t(\mathbf{p}) = \frac{1}{L} \sum_{l=1}^L f_{l,t}(\mathbf{p})$  ▷ Gaussian mixture function
9:   if  $f_t(\hat{\mathbf{p}}_c) < \Lambda$  then
10:    IsAttack = True
11:   else
12:    IsAttack = False
13:   end if
14: end for

```

---

Our scheme consists of two key components: subset generation for positioning and location fusion for spoofing detection. The overall procedure is shown as Algorithm 1.

The first component (Sec. V-B) of our scheme collects ranging information in real-time from multiple infrastructures, including GNSS, Wi-Fi, and cellular networks. For different infrastructures, subsets are generated as combinations of ranging information. Note that GNSS includes GPS, Galileo, and so on, so we can also see them as different infrastructures. The size of the subsets is from the minimal measurements required by the positioning algorithm to the maximum. Then, it computes temporary locations with uncertainty for each subset and infrastructure individually.

The second component (Sec. V-C) utilizes onboard sensors to collect speed, acceleration, and attitude data, which is used to assist in the refinement of temporary locations obtained from the first component. The filtering procedure smooths the locations according to the motion constraints of the receiver. The filtered locations are then fused with the resultant positioning uncertainty, and the composite likelihood function is normalized to derive the final likelihood function utilized for GNSS spoofing detection.

### B. Subset Generation

The first component, subset generation, is actually a resampling method that selects different subsets of all the ranging information, similar to cross-validation.

1) *Raw Data Collection*: The input raw data are pseudoranges, SOPs (providing distance estimates of the device from the corresponding terrestrial infrastructure elements (anchors)), and motion measurements. Pseudoranges are not actual distances between satellites and the GNSS receivers and are often estimated using the time the navigation signals take to propagate in the sky, which have random and systematic clock errors. SOPs from Wi-Fi and cellular anchors contain RSSI, signal-to-noise

ratio (SNR), time-of-arrival (TOA), and radio type. These values, even though they are not actual distances, are related to distances, forming the fundamental basis for positioning algorithms:

- Pseudorange is an approximation of the distance measurement between a satellite and a GNSS receiver. The pseudorange for each satellite is the time (the signal takes to reach the receiver) multiplied by the speed of light:  $\rho = c\Delta t$ . However, because the quartz oscillator of the receiver clock is not accurate enough, the error may be hundreds of meters after one second, i.e., not the actual distance. Fortunately, the clock is used to measure the pseudoranges at the same time, so all pseudoranges have the same clock error. By finding the pseudoranges of at least four anchors, the clock error can be estimated.
- SOPs can be used for both direct and indirect positioning algorithms, such as Geolocation (Mozilla, 2023), fingerprint-based, and range-based localizations. Geolocation localization directly uses RSSI (as well as SNR and signal frequency if available), based on which weighted nonlinear least squares estimate the location of the receiver. Range-based localization (W. Liu & Chen, 2021) needs the approximations of the distances between BSs/APs and the receiver. RSSI can estimate the distance between a BS/AP and the receiver based on the RSSI and the path loss model. The path loss model accounts for large-scale fading and random noise. The large-scale fading is stable and can be measured in advance in an environment. Random noise can be reduced by multiple measurements and least squares. The receiver can be located by finding the distances of at least three BSs/APs.

2) *Size and Combination:* As we do not have any assumption on the number of falsified ranges, the sizes and combinations of generated subsets should explore all possibilities, from the minimum required by positioning to the maximum: For GNSS, three pseudoranges from satellites will determine the location. latitude, longitude, and height, while the fourth one will synchronize the receiver clock. For BSs/APs, at least three distances can determine the receiver location and the clock error has relatively little effect. Thus, the sizes of subsets are  $C(J_1, 4) + C(J_1, 5) + \dots + C(J_1, J_1)$  for GNSS,  $C(J_m, 3) + C(J_m, 4) + \dots + C(J_m, J_m)$ ,  $m \in \{2, 3\}$  for Wi-Fi and cellular networks, and the total number of subsets is denoted as  $L$ . Additionally, if necessary, we can further categorize the information from GPS, Galileo, 2G, 5G, etc, as distinct types.

3) *Positioning Methods:* For computing temporary locations from subsets of ranging information, various methods such as time difference of arrival (TDOA), multilateration, and weighted nonlinear least squares are employed exclusively for their targeted data.

- TDOA localization uses the difference of distances to locate the mobile platform, which solves a number of hyperbolic equations:

$$\rho_j^m(t) - \rho_k^m(t) = \|\mathbf{p}_j^m(t) - \hat{\mathbf{p}}_c(t)\|_2 - \|\mathbf{p}_k^m(t) - \hat{\mathbf{p}}_c(t)\|_2, \forall j, k \quad (1)$$

If we would like to estimate time, substitute  $\rho = c\Delta t$  into the above.

- Distance-based multilateration localization uses multiple distances between the mobile platform and multiple BSs/APs with known locations:

$$\rho_j^m(t) = \|\mathbf{p}_j^m(t) - \hat{\mathbf{p}}_c(t)\|_2, \forall j \quad (2)$$

- Geolocation localization uses weighted nonlinear least squares to minimize the weighted sum of the squared distances between BSs/APs and the estimated location. The weights are inversely proportional to the squared signal strengths (Mozilla, 2023).

$$\min_{\hat{\mathbf{p}}_c(t)} \sum_j \left( \frac{\|\mathbf{p}_j^m(t) - \hat{\mathbf{p}}_c(t)\|_2}{\rho_j^m(t)} \right)^2 \quad (3)$$

Each subset computes an estimated location of the mobile platform  $\mathbf{p}_l(t)$ , where  $l = 1, 2, \dots, L$  and  $L$  is the total number of subsets.

### C. Location Fusion

The second component, location fusion, utilizes signal processing techniques to estimate the likelihood of GNSS spoofing.

1) *Motion Information:* We use  $\mathbf{p}_l(t)$  from the previous component and  $\mathbf{v}(t)$ ,  $\mathbf{a}(t)$  from onboard sensors as input data and local polynomial regression to filter the noise.

The state of mobile platform,  $(\mathbf{p}_l(t), \mathbf{v}(t), \mathbf{a}(t))$ ,  $l = 1, 2, \dots, L$ , evolved from  $t - 1$ , so:

$$\mathbf{p}_l(t) = \mathbf{p}_l(t - 1) + \mathbf{v}(t - 1) + \frac{1}{2}\mathbf{a}(t - 1) \quad (4)$$

$$\mathbf{v}(t) = \mathbf{v}(t - 1) + \mathbf{a}(t - 1) \quad (5)$$

and the state transition matrix is:

$$\mathbf{F}(t) = \begin{bmatrix} 1 & 1 \\ 0 & 1 \end{bmatrix} \quad (6)$$

and the control-input matrix is  $\mathbf{B}(t) = \begin{bmatrix} \frac{1}{2} & 1 \end{bmatrix}^T$ . We conclude that  $(\mathbf{p}_l(t), \mathbf{v}(t)) = \mathbf{F}(t - 1) \cdot (\mathbf{p}_l(t - 1), \mathbf{v}(t - 1)) + \mathbf{B}(t - 1) \cdot \mathbf{a}(t - 1) + \mathbf{n}$ , where  $\mathbf{n}$  models noise.

Then, for filtering the noise, we use an estimator  $\hat{\mathbf{p}}_l(t) = \mathbf{W}\mathbf{t}$ , where  $\mathbf{W} \in \mathbb{R}^{2 \times (n+1)}$  is a matrix of polynomial coefficients,  $\mathbf{t}$  is a  $(n+1)$  dimensional vector and  $[\mathbf{t}]_i = t^{i-1}$ , and  $\mathbf{W}$  is from the local polynomial regression problem:

$$\begin{aligned} \min_{\mathbf{W}} \quad & \sum_{t=t'-w}^{t'-1} [\mathbf{W}\mathbf{t} - \mathbf{p}_l(t)]^\top K_{\text{loc}}(t-t') [\mathbf{W}\mathbf{t} - \mathbf{p}_l(t)] \\ \text{s.t.} \quad & |\mathbf{W}\mathbf{t}' - \mathbf{p}_l(t'-1)| \leq \epsilon \end{aligned} \quad (7)$$

where  $w$  is a rolling window of the filter and  $\epsilon \in \mathbb{R}^2$  in the constraint is a small tolerance. After solving the problem, we have  $\hat{\mathbf{p}}_l(t)$ .

2) *Uncertainty Modelling*: We have different cases: (i) For statistical positioning techniques, the covariance matrix from the positioning process derives confidence intervals; (ii) For other positioning techniques, we use the residual vector from the local polynomial regression in (7) to model the uncertainty of estimated locations  $\hat{\mathbf{p}}_l(t)$ .

In case (i), dilution of precision (DOP) derived from the covariance matrix of statistical positioning techniques serves as a direct indicator of the uncertainty associated with positioning results. To illustrate, the position DOP can be determined by considering the diagonal elements of the covariance matrix obtained via the least squares method. This value is often correlated with the standard deviation  $\sigma_l(t)$  of  $\hat{\mathbf{p}}_l(t)$ .

In case (ii), the residual part between  $\mathbf{p}_l(t)$  and  $\hat{\mathbf{p}}_l(t)$  from  $l$ th subset at time  $t$  is

$$\mathbf{d}_l(t) = \hat{\mathbf{p}}_l(t) - \mathbf{p}_l(t). \quad (8)$$

Then, the uncertainty is the standard deviation  $\sigma_l(t)$ ,

$$(\sigma_l(t))^2 = \frac{1}{L} \sum_{l=1}^L \left( \mathbf{d}_l(t) - \frac{1}{L} \sum_{i=1}^L \mathbf{d}_i(t) \right)^2 \quad (9)$$

and thus the probability density function is  $f_{l,t}(\mathbf{p}) = \frac{1}{\sigma_l(t)\sqrt{2\pi}} \exp\left(-\frac{1}{2} \frac{(\mathbf{p} - \hat{\mathbf{p}}_l(t))^2}{\sigma_l(t)^2}\right)$ , where the operations are point-wise.

3) *Gaussian Mixture*: The Gaussian mixture function fuses temporary locations with uncertainties derived from the subsets. So far we have locations  $\hat{\mathbf{p}}_l(t)$  associated with uncertainty  $\sigma_l(t)$ , which are assumed to follow distributions  $\mathcal{N}(\hat{\mathbf{p}}_l(t), \sigma_l(t))$ . At time  $t$ , the Gaussian mixture for  $l = 1, 2, \dots, L$  can be represented as:

$$\begin{aligned} f_t(\mathbf{p}) &= \frac{1}{L} \sum_{l=1}^L f_{l,t}(\mathbf{p}) \\ &= \frac{1}{L} \sum_{l=1}^L \frac{1}{\sigma_l(t)\sqrt{2\pi}} \exp\left(-\frac{1}{2} \frac{(\mathbf{p} - \hat{\mathbf{p}}_l(t))^2}{\sigma_l(t)^2}\right) \end{aligned}$$

which serves as a likelihood function; specifically, it represents the likelihood of the original GNSS computed position  $\hat{\mathbf{p}}_c$  not being under attack, denoted as  $f_t(\hat{\mathbf{p}}_c)$ . To make a decision, a threshold  $\Lambda$  is predefined, and if  $f_t(\hat{\mathbf{p}}_c)$  is less than  $\Lambda$ , an alarm will be raised. If an attack is detected, the proposed scheme would take the value under the maximum likelihood of the mixture function  $f_t(\mathbf{p})$  to recover the actual position:  $\hat{\mathbf{p}}_c(t) = \arg \max_{\mathbf{p}} f_t(\mathbf{p})$ .

#### D. Theoretical Analysis

To facilitate the analysis of the overall algorithm performance, we assign zero values to random errors while retaining the deviation induced by the attacker. Additionally, in our scenario, we consider that the satellite geometry and the geometry of other anchors for positioning are not poor. Furthermore, we categorize the attacks into (i) *Coordinated Attack*, where the spoofed ranging information (across all available infrastructures) is collectively designed with a specific spoofing position in mind, and (ii) *Uncoordinated Attack* otherwise (the spoofed ranging information is independently (possibly randomly) chosen).

1) *GNSS-only Case*: For multilateration algorithm used by GNSS positioning, at least 4 satellites are needed to determine coordinates and local clock error, so we denote  $N_{\min} = 4$  as the minimum satellite number. Similarly,  $N_{\text{sat}}$  is the total number of satellites providing pseudoranges and  $N_{\text{adv}}$  is the number of pseudoranges with deviations induced by the attacker.

**Lemma 1.** Suppose that  $N_{\text{sat}} - N_{\text{adv}} > N_{\min}$ . Then, we can recover  $\mathbf{p}_c$  from an Uncoordinated Attack.

**Proposition 1.** Suppose that  $N_{\text{sat}} - N_{\text{adv}} \geq N_{\min}$ . Then, we can detect an Uncoordinated Attack.

**Corollary 1.** An adversarial subset can contain at most  $N_{\min} - 1$  benign pseudoranges without being detected.

**Lemma 2.** Suppose that  $\sum_{i=N_{\min}}^{N_{\text{sat}}-N_{\text{adv}}} C(N_{\text{sat}} - N_{\text{adv}}, i) > \sum_{i=1}^{N_{\text{adv}}} C(N_{\text{adv}}, i) \sum_{j=N_{\min}-i}^{N_{\min}-1} C(N_{\min} - 1, j)$ .<sup>1</sup> Then, we can recover  $\mathbf{p}_c$  from a Coordinated Attack.

This represents a classical Multiple Fault Detection and Exclusion. For the detailed proof process, please consult the single constellation case in Zhang and Papadimitratos (2021).

<sup>1</sup>When  $A > B$ , the term  $\sum_{i=A}^B \cdot$  takes value 1.

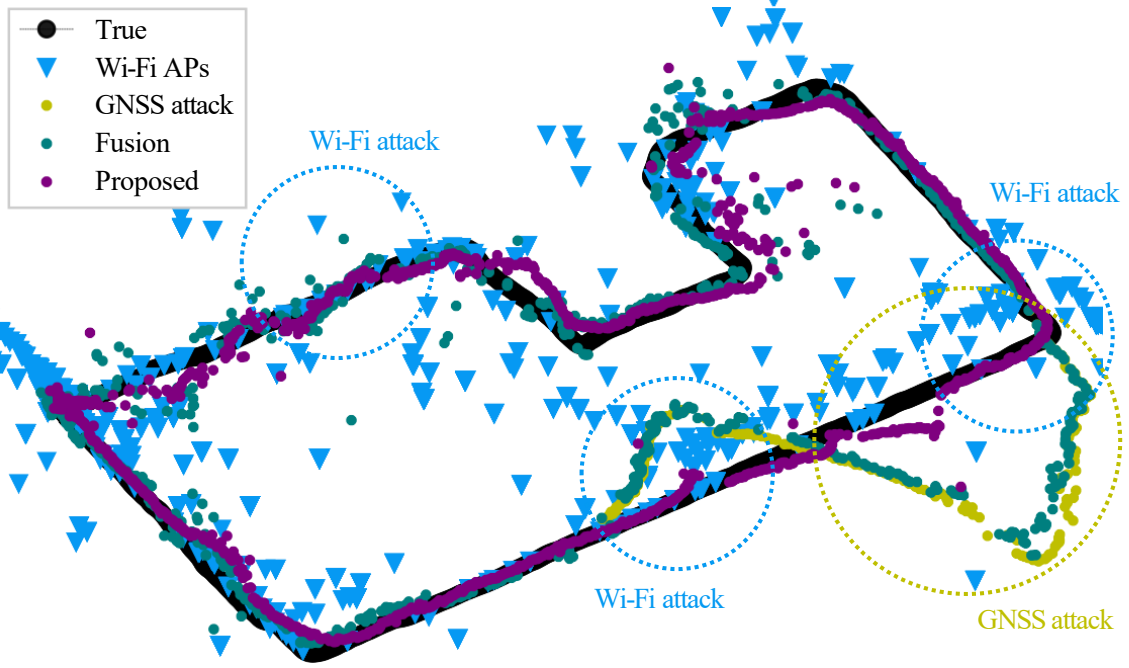


Fig. 3: An illustration of the attack-induced deviations and the recovered locations from the proposed method.

2) *Multi-infrastructure Case*: Most distance-based multilateration algorithms for network-based positioning need at least 3 anchors (i.e., BSs and APs) to determine the coordinates of the receiver. We denote  $N_{\min}^m$  as the minimum anchor number required by the positioning for  $m$ th infrastructure,  $N_{\text{anc}}^m$  as the total number of anchors providing ranging information, and  $N_{\text{adv}}^m$  as the number of anchors affected by an attacker thus providing adversarial ranging information.

**Theorem 1.** Suppose that  $\exists m$ , s.t.  $N_{\text{anc}}^m - N_{\text{adv}}^m > N_{\min}^m$ . Then, we can recover  $\mathbf{p}_c$  from an Uncoordinated Attack.

**Theorem 2.** Suppose that  $\sum_{m=1}^M \sum_{i=N_{\min}^m}^{N_{\text{anc}}^m - N_{\text{adv}}^m} C(N_{\text{anc}}^m - N_{\text{adv}}^m, i) > \sum_{m=1}^M \sum_{i=1}^{N_{\text{adv}}^m} C(N_{\text{adv}}^m, i) \sum_{j=N_{\min}^m - i}^{N_{\min}^m - 1} C(N_{\min}^m - 1, j)$ . Then, we can recover  $\mathbf{p}_c$  from a Coordinated Attack.

Intuitively, the conditions of the multi-infrastructure case are easier to satisfy than GNSS-only case, so the detector using multi-infrastructure is stronger. We provide a proof sketch: Leveraging the Lemmas derived from the GNSS-only scenario, we implement Multiple Fault Detection and Exclusion similar to the case of a single constellation, for each infrastructure within multi-infrastructures separately. The results from both individual subsets and infrastructures are then aggregated. Successful detection and exclusion are feasible as long as the benign subsets outnumber the attack(er) subsets.

## VI. EXPERIMENTS

We study a dataset combining GNSS with untrusted opportunistic information, in which the trace is collected in the real world and the attacks are synthesized based on real data. Then, we evaluate the true positive probability of attack detection.

### A. Dataset

The raw GNSS measurements are collected using Google Pixel 4 XL phone and GNSSLogger (Fu, Khider, & van Diggelen, 2020) in the Android system, and contain a walking trace at the Kista Science City. This dataset also incorporates data from onboard sensors, such as IMU, and wireless networks, including cellular and Wi-Fi, with details such as names, RSSI, and unique IDs. The latitude and longitude information of APs and BSs is sourced from Wigle (Bobilla, Arkasha, & Uhtu, 2023). Positioning algorithms employed include weighted least squares for GNSS and weighted nonlinear least squares for network infrastructures.

For GNSS spoofing, instead of spoofing the mobile phone, the attack is synthesized by modifying the raw GNSS data. We gradually increase the pseudorange of two satellites, causing the derived location to deviate progressively from the actual one. Additionally, three rogue Wi-Fi APs are synthesized and strategically “placed” near some locations of the trace to broadcast signals to simulate APs from a different fixed location, which causes 600 spoofed Wi-Fi RSSI measurements/values. The GNSS

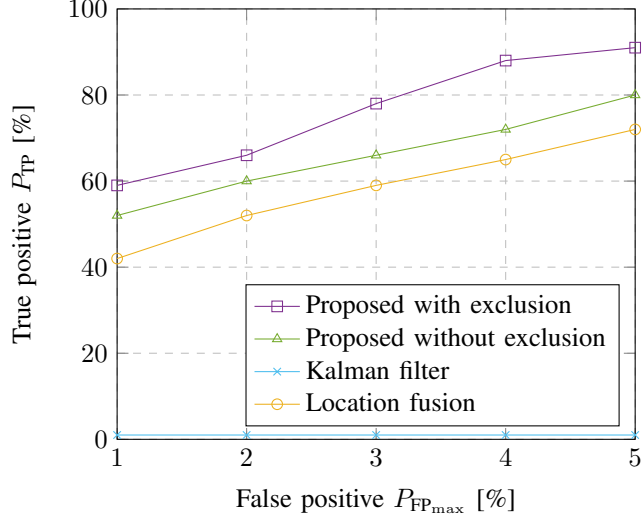


Fig. 4:  $P_{TP}$  of the proposed method (with/without exclusion), Kalman filter, and location fusion-based detector.

spoofing spans 130 seconds, while simulated signals from rogue Wi-Fi APs last around 120 seconds, with the entire trace extending over 1030 seconds. The GNSS spoofing deviation gradually increases from 0 to 145 meters and then decreases to 0 meters illustrated by Fig. 3.

### B. Baseline Methods

To assess the performance improvement of the proposed RAIM, we compare it with baseline methods:

- **Kalman filter:** This method utilizes filtering based on IMU information in conjunction with GNSS locations. It calculates the distance between the filtered location and the original GNSS location. If the distance exceeds a specified threshold, a spoofing alarm is triggered.
- **Location fusion:** In scenarios where the mobile platform cannot obtain detailed ranging information like pseudoranges from the GNSS receiver, and thus cannot generate pseudorange subsets for RAIM, this method directly acquires GNSS-provided locations and location estimations from network infrastructures. Subsequently, a fusion method (W. Liu & Papadimitratos, 2023) is employed to calculate an ultimate location with uncertainty for detection.

### C. Detection Result

Recall that our problem is maximizing the true positive probability of spoofing detection,  $P_{TP}$ , when fixing false positive,  $P_{FP_{max}}$ . We choose different  $P_{FP_{max}}$  and evaluate  $P_{TP}$ . We also test two different strategies to construct the Gaussian mixture function, i.e., with and without outlier subset exclusion. If the distance between the temporary location  $\hat{p}_l(t)$ ,  $l = 1, 2, \dots, L$  and  $\hat{p}_c(t)$  is larger than a threshold value, then the exclusion strategy will drop the temporary location  $\hat{p}_l(t)$ .

In the presence of an attacker-designed GNSS trace, as in Fig. 3, and attacker-replayed SOPs in the dataset, our proposed scheme exhibits a detection performance improvement of over 60% compared to the Kalman filter as depicted in Fig. 4. One key factor contributing to this enhancement is our algorithm's integration of both onboard sensors and terrestrial network infrastructures, whereas the Kalman filter incorporates only IMU data. When compared to the location fusion approach, our proposed scheme with exclusion exhibits a 10–15% increase in detection performance and a 5–10% gain for the proposed without exclusion. Based on our theoretical analysis in Sec. V-D, this improvement is attributed to our algorithm's utilization of detailed ranging information instead of relying solely on direct location data. Notably, our approach distinguishes itself by incorporating heterogeneous data, checking for inconsistencies, and avoiding the assumption that redundant wireless signals are inherently benign as references.

In addition, through an internal comparison between the proposed method with outlier subset exclusion and the proposed method without outlier subset exclusion, we observe a performance gain of 5–10% attributable to the outlier exclusion strategy in our RAIM. This gain is achieved by automatically eliminating subsets with temporary locations that are more than a threshold distance (around 150 meters in our setting) away from the peak of the Gaussian mixture function. This exclusion effectively minimizes the negative impact of fault subsets on the construction of the Gaussian mixture function.

Fig. 3 shows the proposed recovered location, i.e., the peak of the Gaussian mixture function, from the proposed method, in which we can observe that it is resisted to gradual deviation attack in the presence of rogue APs/BSs. Fig. 5 is the relation between likelihood,  $f_t(\hat{p}_c)$ , false positive probability,  $P_{FP_{max}}$ , and true positive probability,  $P_{TP}$ . We notice that by setting the likelihood threshold to a relatively high value,  $P_{TP}$  can be very high while maintaining a low  $P_{FP_{max}}$ ; which implies that the alarm should be triggered only if the likelihood of spoofing is high.

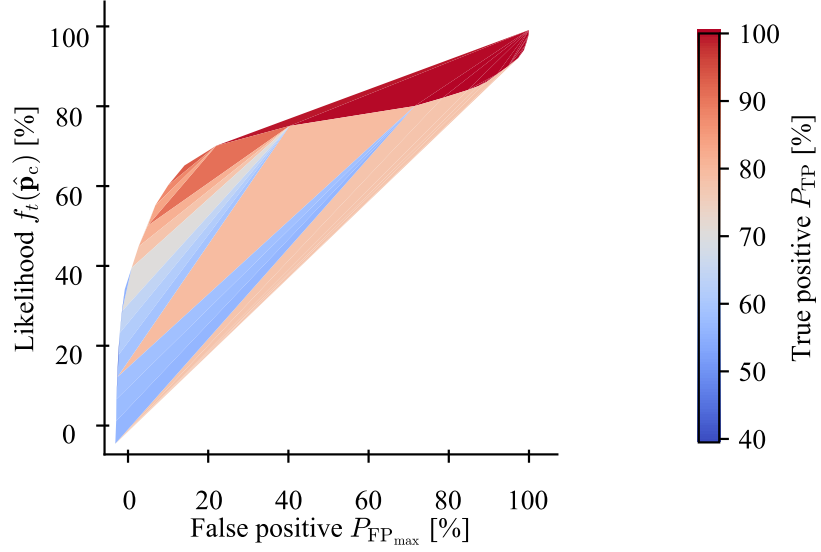


Fig. 5: A plot of the relation between likelihood,  $f_t(\hat{\mathbf{p}}_c)$ , false positive probability,  $P_{FP_{max}}$ , and true positive probability,  $P_{TP}$ .

## VII. CONCLUSION

The paper proposed a Gaussian mixture RAIM for detecting GNSS spoofing by using multiple sources of untrusted information such as ranging information, speed, and acceleration. The system collects data from GNSS, Wi-Fi, cellular networks, and onboard sensors, generates subsets of ranging information for each infrastructure, computes temporary locations for each subset using a positioning algorithm, filters the locations using onboard sensors, models their uncertainty with statistics, and fuses them to assess the likelihood of GNSS spoofing. The approach consists of two key components: subset generation for positioning and location fusion for spoofing detection. The simulation and numerical results show a more than 90% true positive detection rate under 5% false alarm.

In the continuation of this work, our attention will be directed towards enhancing accuracy, efficiency, and conducting further experiments. To elevate location and detection accuracy, we will introduce various strategies for excluding abnormal information. In terms of computational efficiency, we plan to propose sampling methods for subsets and provide theoretical evidence of their performance equivalence with/without sampling. Additionally, we aim to refine our theoretical analysis and conduct additional experiments in both simulators and real-world environments.

## REFERENCES

- Anderson, J. M., Carroll, K. L., DeVilbiss, N. P., Gillis, J. T., Hinks, J. C., O'Hanlon, B. W., ... Yazdi, R. A. (2017, September). Chips-message robust authentication (chimera) for GPS civilian signals. In *Proc. 30th ION GNSS+*. Portland, OR, USA.
- Blanch, J., Walker, T., Enge, P., Lee, Y., Pervan, B., Rippl, M., ... Kropp, V. (2015). Baseline advanced RAIM user algorithm and possible improvements. *IEEE Trans. Aerosp. Electron. Syst.*, 51(1), 713–732.
- Bobzilla, Arkasha, & Uhtu. (2023). Wigle.net. all the networks. found by everyone. *WiGLE*. Retrieved 2023-09-15, from <https://wigle.net/>
- Brown, R. G. (1992). A baseline GPS RAIM scheme and a note on the equivalence of three RAIM methods. *J. Inst. Navigation*, 39(3), 301–316.
- Fu, G. M., Khider, M., & van Diggelen, F. (2020, September). Android raw GNSS measurement datasets for precise positioning. In *Proc. 33rd ION GNSS+*. virtual event.
- Gao, Y., & Li, G. (2022). A slowly varying spoofing algorithm avoiding tightly-coupled GNSS/IMU with multiple anti-spoofing techniques. *IEEE Trans. Veh. Technol.*, 71(8), 8864–8876.
- Gao, Y., & Li, G. (2023). Two time spoofing algorithms on GNSS receiver instrumentation of modifying satellite clock correction parameters in navigation message. *IEEE Trans. Instrum. Meas.*, 72, 1–11.

- GMV. (2023a). Galileo open service navigation message authentication. *Navipedia*. Retrieved 2023-03-03, from <https://gssc.esa.int/navipedia/index.php/Galileo-Open-Service-Navigation-Message-Authentication>
- GMV. (2023b). GNSS authentication and encryption. *Navipedia*. Retrieved 2023-03-03, from <https://gssc.esa.int/navipedia/index.php/GNSS-Authentication-and-encryption>
- Goodin, D. (2022). GPS interference caused the FAA to reroute Texas air traffic. experts stumped. *Ars Technica*. Retrieved 2022-10-20, from <https://arstechnica.com/information-technology/2022/10/cause-is-unknown..>
- Humphreys, T. E., Ledvina, B. M., Psiaki, M. L., O'Hanlon, B. W., Kintner, P. M., et al. (2008, September). Assessing the spoofing threat: Development of a portable GPS civilianspoof. In *Proc. 21st ION GNSS+*. Savannah, GA, USA.
- Joerger, M., Chan, F.-C., & Pervan, B. (2014). Solution separation versus residual-based RAIM. *J. Inst. Navigation*, 61(4), 273–291.
- Kassas, Z. M., Khalife, J., Abdallah, A. A., & Lee, C. (2022). I am not afraid of the GPS jammer: Resilient navigation via signals of opportunity in GPS-denied environments. *IEEE Aerosp. Electron. Syst. Mag.*, 37(7), 4-19.
- Khanafseh, S., Roshan, N., Langel, S., Chan, F.-C., Joerger, M., & Pervan, B. (2014, May). GPS spoofing detection using RAIM with INS coupling. In *Proc. IEEE/ION PLANS*. Monterey, CA, USA.
- Lenhart, M., Spanghero, M., & Papadimitratos, P. (2022, January). Distributed and mobile message level relaying/replaying of GNSS signals. In *Proc. ION ITM* (pp. 56–67). Long Beach, CA, USA.
- Liu, S., Cheng, X., Yang, H., Shu, Y., Weng, X., Guo, P., ... Yang, Y. (2021, August). Stars can tell: A robust method to defend against GPS spoofing attacks using off-the-shelf chipset. In *Proc. 30th USENIX Security*. virtual event.
- Liu, W., & Chen, J. (2021). UAV-aided radio map construction for wireless communications and localization. *arXiv preprint arXiv:2107.10574v1*.
- Liu, W., & Papadimitratos, P. (2023, April). Probabilistic detection of GNSS spoofing using opportunistic information. In *Proc. IEEE/ION PLANS*. Monterey, CA, USA.
- Maaref, M., & Kassas, Z. M. (2021). Autonomous integrity monitoring for vehicular navigation with cellular signals of opportunity and an IMU. *IEEE Trans. Intell. Transp. Syst.*, 23(6), 5586–5601.
- Maier, D., Frankl, K., Blum, R., Eissfeller, B., & Pany, T. (2018, April). Preliminary assessment on the vulnerability of NMA-based galileo signals for a special class of record & replay spoofing attacks. In *Proc. IEEE/ION PLANS*. Monterey, CA, USA.
- Mozilla. (2023). *Ichnaea*. <https://github.com/mozilla/ichnaea/blob/main/ichnaea/api/locate/mac.py>. GitHub.
- Narain, S., Ranganathan, A., & Noubir, G. (2019, May). Security of GPS/INS based on-road location tracking systems. In *Proc. IEEE S&P*. San Francisco, CA, USA.
- Olieri, G., Sciancalepore, S., Ibrahim, O. A., & Di Pietro, R. (2022). GPS spoofing detection via crowd-sourced information for connected vehicles. *Comput. Netw.*, 216, 109230.
- Ranganathan, A., Ólafsdóttir, H., & Capkun, S. (2016, October). SPREE: A spoofing resistant GPS receiver. In *Proc. 22nd ACM MobiCom*. New York, NY, USA.
- Roysdon, P. F., & Farrell, J. A. (2017, May). GPS-INS outlier detection & elimination using a sliding window filter. In *Proc. Am. Control Conf.* Seattle, WA, USA.
- Saedi, M., Moore, A., Perry, P., Shojafar, M., Ullah, H., Synnott, J., ... Herwono, I. (2020, June). Generation of realistic signal strength measurements for a 5G rogue base station attack scenario. In *Proc. IEEE CNS*. Avignon, France.
- Sathaye, H., Strohmeier, M., Lenders, V., & Ranganathan, A. (2022, August). An experimental study of GPS spoofing and takeover attacks on UAVs. In *Proc. 31st USENIX Security*. Boston, MA, USA.
- Shaik, A., Borgaonkar, R., Park, S., & Seifert, J.-P. (2018, June). On the impact of rogue base stations in 4G/LTE self organizing networks. In *Proc. 11th ACM WiSec*. Stockholm, Sweden.
- Shen, J., Won, J. Y., Chen, Z., & Chen, Q. A. (2020, August). Drift with devil: Security of multi-sensor fusion based localization in high-level autonomous driving under GPS spoofing. In *Proc. 29th USENIX Security*. virtual event.
- Shi, Y., Davaslioglu, K., & Sagduyu, Y. E. (2020). Generative adversarial network in the air: Deep adversarial learning for wireless signal spoofing. *IEEE Trans. Cogn. Commun. Netw.*, 7(1), 294–303.
- Spanghero, M., & Papadimitratos, P. (2023, April). Detecting GNSS misbehavior leveraging secure heterogeneous time sources. In *Proc. IEEE/ION PLANS*. Monterey, CA, USA.
- Vanhoef, M., & Piessens, F. (2017, October). Key reinstallation attacks: Forcing nonce reuse in WPA2. In *Proc. ACM CCS*. Dallas, TX, USA.
- Werner, D. (2022). HawkEye 360 detects GPS interference in Ukraine. *SPACENEWS*. Retrieved 2022-10-20, from <https://spacenews.com/hawkeye-360-gps-ukr/>
- Wesson, K., Rothlisberger, M., & Humphreys, T. (2012). Practical cryptographic civil GPS signal authentication. *J. Inst. Navigation*, 59(3), 177–193.

- Yan, D., Yan, Y., Yang, P., Song, W.-Z., Li, X.-Y., & Liu, P. (2022). Real-time identification of rogue WiFi connections in the wild. *IEEE Internet Things J.*, 10(7), 6042–6058.
- Zhang, K., Larsson, E. G., & Papadimitratos, P. (2022). Protecting GNSS open service navigation message authentication against distance-decreasing attacks. *IEEE Trans. Aerosp. Electron. Syst.*, 58(2), 1224–1240.
- Zhang, K., & Papadimitratos, P. (2019a, January). On the effects of distance-decreasing attacks on cryptographically protected GNSS signals. In *Proc. ION ITM*. Reston, VA, USA.
- Zhang, K., & Papadimitratos, P. (2019b, March). Secure multi-constellation GNSS receivers with clustering-based solution separation algorithm. In *Proc. IEEE Aerosp. Conf.* Big Sky, MT, USA.
- Zhang, K., & Papadimitratos, P. (2021). Fast multiple fault detection and exclusion (FM-FDE) algorithm for standalone GNSS receivers. *IEEE Open J. Commun. Soc.*, 2, 217–234.
- Zhang, K., Tuhin, R. A., & Papadimitratos, P. (2015, November). Detection and exclusion RAIM algorithm against spoofing/replaying attacks. In *Proc. Int. Symp. GNSS*. Kyoto, Japan.